JTTEE5 19:495–501
DOI: 10.1007/s11666-009-9416-0
1059-9630/$19.00 © ASM International

Thin and Dense Ceramic Coatings by Plasma Spraying at Very Low Pressure

Georg Mauer, Robert Vaßen, and Detlev Stöver

(Submitted March 31, 2009; in revised form July 28, 2009)

The very low pressure plasma spray (VLPPS) process operates at a pressure range of approximately 100 Pa. At this pressure, the plasma jet interaction with the surrounding atmosphere is very weak. Thus, the plasma velocity is almost constant over a large distance from the nozzle exit. Furthermore, at these low pressures the collision frequency is distinctly reduced and the mean free path is strongly increased. As a consequence, at low pressure the specific enthalpy of the plasma is substantially higher, but at lower density. These particular plasma characteristics offer enhanced possibilities to spray thin and dense ceramics compared to conventional processes which operate in the pressure range between 5 and 20 kPa. This paper presents some examples of gas-tight and electrically insulating coatings with low thicknesses <50 µm for solid oxide fuel cell applications. Furthermore, plasma spraying of oxygen conducting membrane materials such as perovskites is discussed.

Keywords Al-Mg-spinel, gas separation, insulating layer, low pressure plasma spraying (LPPS), membrane, perovskite, SOFC

1. Introduction

The very low pressure plasma spray (VLPPS) process has been developed with the aim of depositing uniform and thin coatings with large area coverage by plasma spraying. At typical pressures of 100-200 Pa, the characteristics of the plasma jet change compared to conventional low pressure plasma spraying processes (LPPS) operating at 5-20 kPa. Enthalpy probe measurements (Ref 1) show that the plasma jet extends much larger in the axial as well as in the radial direction. Typical dimensions are >1 m in length and >0.2 m in diameter depending on the parameters. Accordingly, the profiles of specific enthalpies and temperature change only slightly over a large range of the axial spray distance and are also broadened in the radial direction. Furthermore, the specific enthalpy and temperature on the jet axis are enhanced. The plasma velocities are also distinctly dependant on the pressure. The lower the pressure, the higher the velocity level becomes and the velocity is almost constant over the axial distance. Similarly, the radial velocity profiles are broadened as pressure is decreased.

This article is an invited paper selected from presentations at the 2009 International Thermal Spray Conference and has been expanded from the original presentation. It is simultaneously published in *Expanding Thermal Spray Performance to New Markets and Applications: Proceedings of the 2009 International Thermal Spray Conference*, Las Vegas, Nevada, USA, May 4-7, 2009, Basil R. Marple, Margaret M. Hyland, Yuk-Chiu Lau, Chang-Jiu Li, Rogerio S. Lima, and Ghislain Montavon, Ed., ASM International, Materials Park, OH, 2009.

Georg Mauer, Robert Vaßen, and **Detlev Stöver**, Forschungszentrum Jülich GmbH, Institut für Energieforschung IEF-1, 52425 Jülich, Germany. Contact e-mail: g.mauer@fz-juelich.de.

2. Literature Review

Enthalpy probe measurements clearly show that at lower ambient pressure the plasma jet becomes supersonic. This means that the plasma gas can exit the nozzle at a pressure which is different from the chamber pressure. As the flow is faster than the pressure waves traveling in the plasma at the local speed of sound, no information on the chamber pressure is communicated inside the nozzle (Ref 2). If the exit pressure of the jet is lower than the chamber pressure it is over-expanded showing typical luminous oblique shock waves originating from the edge of the nozzle and forming subsequent compression and expansion cells indicating that the jet local static pressure is brought to the chamber pressure level. However, in the VLPPS process the ambient pressure is significantly below the exit pressure of the jet. Thus, it becomes under-expanded showing a hot and dense plume exiting the nozzle. The jet length increases as the chamber pressure is decreased (Ref 3) and the subsequent expansion zone being associated with a drop in temperature and pressure moves downstream.

Enthalpy probe measurements showed that the axial temperature profile of the plasma jet is at higher level and more uniform compared to conventional spray processes at higher chamber pressures. One reason for the more uniform temperature and velocity distribution and their raised levels is the laminar flow of the plasma. Therefore, the interaction of the plasma jet with the surrounding low density atmosphere is weak consequently it is cooled and

decelerated less. Moreover, in the plasma jet the mean free path is increased and accordingly the collision frequency is reduced. This is indicated by a reduction of the continuum emission which is a sign of fewer recombination processes. As a consequence, the specific enthalpy of the plasma is substantially higher at low pressure (Ref 1). However, it has also to be considered, that the density and viscosity of the plasma jet are lowered so that the thermal transfer to particles and the deposition efficiency are affected. Therefore, the grain size distribution of the powder feedstock preferably has to be reduced (Ref 4).

The plasma characteristics at very low pressure are promising with regard to manufacturing of thin, dense, and well-adherent ceramic coatings. The large and uniform energy distribution also allows coating of thin substrates which are sensitive to thermal deformation.

The combination of plasma spraying at low pressures with enhanced electrical input power has led to the development of the LPPS-TF™ process (TF = thin film). Applying the O3CP gun (Sulzer Metco, Wohlen, Switzerland) at electrical currents up to 2.5 kA an input power level of 150 kW is achieved (Ref 5). At appropriate parameters, it is even possible to evaporate the powder feedstock material providing advanced microstructures of the deposits (Ref 6). However, in this study the conventional F4 gun (Sulzer Metco, Wohlen, Switzerland) was used as it was the gun which was available at the time. It can be operated up to 55 kW input power. The F4 has already been applied at low pressures as reported in Ref 4. To distinguish this process from the LPPS-TF™ process as well as from the conventional LPPS process at much higher pressures, the terminology of VLPPS is used in this paper.

3. Application Fields for Thin and Dense Plasma Sprayed Ceramic Coatings

Plasma sprayed coatings consist of molten or partially molten droplets impacting on a substrate, spreading to thin lamellae which are rapidly cooling down. Thus, especially coatings of high melting ceramics usually show interconnected pores and cracks and hence are not useful for applications in which gas-tightness is essential (Ref 7). Gas permeation through porous plasma sprayed coatings is controlled by two basic mechanisms. In larger globular pores, the mean free path of the permeating gas molecules is small compared to the pore dimensions. In this case, gas permeation shows viscous flow which is characterized by molecule-molecule collisions and can be assumed to be primarily laminar. In contrast, in smaller pores and cracks molecule-wall collisions are predominating. In this so-called Knudsen region, gas permeation occurs due to free molecule flow. Permeation measurements (Ref 8) on plasma sprayed yttria-stabilized zirconia (YSZ) coatings made from different size distribution powders showed the dependence of the gas permeability on the amount of porosity as well as on the pore sizes and furthermore proved the significance of both the mechanisms at different proportions in each case. Hence, gas-tight ceramic coatings are a challenge for plasma spray technology in particular at small layer thicknesses of some tens of micrometers. In the following, two application fields for plasma sprayed dense ceramic coatings are described with their specific requirements.

3.1 Gas Separating Membranes

Perovskite type materials with a high electronic and ionic (“mixed”) conductivity can be used as oxygen ion conducting membranes. They have the potential to play an important role in the CO_2 sequestration technologies in which fuel combustion in pure oxygen is one strategy (Ref 7). In general, perovskite powders decompose easily above their melting temperatures or in reducing atmospheres due to the evaporation or chemical reaction of constituents. As a consequence, in many cases significant fractions of plasma sprayed coatings are non-stoichiometric containing secondary phases affecting the pronounced perovskite conductivity. Thus, plasma spray parameters have to be chosen carefully, in order to limit the heat transfer and the in-flight dwell time to the necessary extent (Ref 9, 10). On the other hand in-flight particle temperatures and velocities must be high enough to provide good deposition efficiency as well as dense coating microstructures even at small coating thickness. Thin coatings are preferred to keep the internal resistance for conducting the electrons and oxygen-ions low. In this paper, VLPPS-sprayed coatings are presented with $Ba_{0.5}Sr_{0.5}Fe_{0.2}Co_{0.8}O_3$ perovskite material which is a new candidate for oxygen ion conducting membranes.

3.2 Solid Oxide Fuel Cells

Solid oxide fuel cells (SOFCs) are one of the options for future energy conversion techniques, e.g., in auxiliary power units (APU) in vehicles or aircrafts (Ref 11). Concerning industrialization of particular metal supported planar cells consisting of metallic frames and substrates coated with the different functional layers are of high interest. Several of them, which require gas-tightness, have the potential to be produced by plasma spraying, for example

- Electrolyte layers of YSZ (Ref 4, 12-16), and
- Electrically insulating layers such as Mg-spinel ($MgAl_2O_4$) on metallic interconnects (Ref 17, 18).

In addition, other functional layers such as anodes, cathodes, and diffusion barriers have also been plasma sprayed (Ref 12-16).

In this paper, electrically insulating Mg-spinel layers produced by VLPPS are presented. In the case of metal supported cells, they are needed to prevent short-circuiting between adjacent support frames. Thus, these layers should maintain sufficient electrical resistance even at SOFC operating temperatures up to 800 °C. Because the frames are brazed for geometrical fixation, the layers should show good wetting and adhesion to the solder. However, as the braze material is electrically conductive,

it is important to prevent it from penetrating into the deposit and causing an electrical short circuit or at least a considerable reduction of the resistance (Ref 17). Furthermore, the insulating layers and braze material have to seal the gas volumes of the cell. In summary, a dense microstructure is an essential feature of plasma sprayed SOFC insulating layers. In addition, they should be preferably thin to prevent cracks and bending due to the thermal mismatch with the substrates. Moreover, an important basic condition is the required planarity of the components which are sensitive for thermal deformation due to their small thickness of approximately 0.5 mm and residual stresses originating from the forming manufacturing.

4. Experimental Procedures

Experiments were carried out on a Sulzer Metco VLPPS Multicoat System. It resulted from a comprehensive reconstruction of an existing conventional LPPS system. In particular, it was equipped with an additional vacuum pumping unit, a large vacuum blower to provide sufficient pumping capacity at low pressures, enlarged cooling capacity, and new control units. Figure 1 gives an overall view of the facility. Presently the F4 gun can be operated. For the nearest future, all preparations are made to apply the TriplexPro gun as soon as a vacuum feasible version is available. Furthermore, additional power sources will be installed to be able then to run also the LPPS-TF™ process with the O3CP gun at elevated power level.

The powder used for the oxygen ion conducting membrane coatings was an in-house spray dried perovskite $Ba_{0.5}Sr_{0.5}Fe_{0.2}Co_{0.8}O_3$ powder. The grain sizes measured by laser diffraction were $d_{10} = 16$ μm, $d_{50} = 41$ μm, and $d_{90} = 103$ μm. Figure 2 shows the particle morphology. As mentioned above, the powder grain sizes should be preferably small for VLPPS operations. Thus, the powder was sieved and only the fraction −45 μm was used. Initially, the substrate material was stainless steel, however for membrane applications, high porous substrates made from the ferrite 26% chromium alloy ITM14 (Plansee, Reutte, Austria) are provided. The substrates were preheated by the plasma jet up to 500 °C immediately before coating.

Table 1 shows the appropriate plasma spray parameters. As reducing atmospheres should be avoided with regard to possible decomposition of the sprayed material, no hydrogen was used as secondary plasma gas. In order to achieve short particle dwell times and high particle in-flight velocities a high argon flow was set for the first sample. In the second parameter set, predominantly helium was used to increase the velocity and to concentrate the plasma jet. Helium has a distinctly higher ionization temperature and the associated drop in viscosity takes place at much higher temperatures compared to argon. This leads to an increased momentum transfer to the particles. As helium and argon are both monatomic gases they show similar enthalpy characteristics. In the third parameter set, nitrogen was introduced as secondary plasma gas. Similar to hydrogen, its enthalpy is considerably higher than of monatomic species due to dissociation.

Fig. 1 VLPPS system at the Institute of Energy Research (IEF-1), Forschungszentrum Jülich GmbH

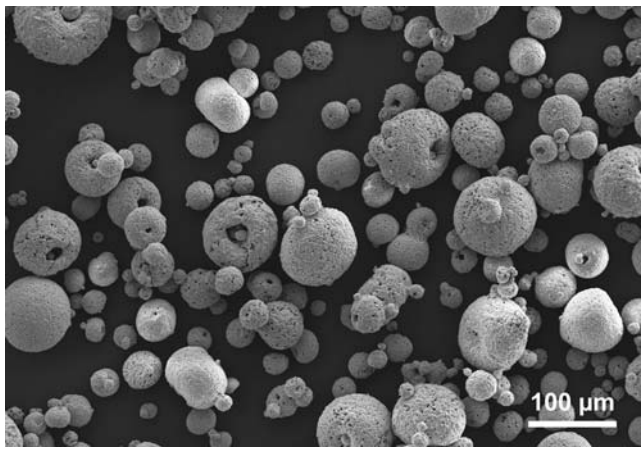

Fig. 2 Morphology of the perovskite $Ba_{0.5}Sr_{0.5}Fe_{0.2}Co_{0.8}O_3$ powder used for the oxygen ion conducting membranes (SEM)

Table 1 Plasma spray parameters applied for the perovskite $Ba_{0.5}Sr_{0.5}Fe_{0.2}Co_{0.8}O_3$ oxygen ion conducting membranes

Plasma gas Ar/N_2/He, input power	(1) 80 slpm/0 slpm/40 slpm, 44.7 kW
	(2) 20 slpm/0 slpm/40 slpm, 31.0 kW
	(3) 50 slpm/8 slpm/0 slpm, 51.2 kW
	(4) 40 slpm/6 slpm/12 slpm, 51.5 kW
	(5) 30 slpm/10 slpm/5 slpm, 51.2 kW
Current	800 A
Atmosphere	150 Pa Ar
Stand-off distance	800 mm

slpm, Standard liters per minute

However, as hydrogen shows highest thermal conductivity, it can be adequately substituted by nitrogen only to limited extent. Finally, two different combinations of N_2 and He with Ar were set to combine the advantages of both the secondary gas species.

The powder being used for the SOFC insulating layers is a commercially available fused and crushed stoichiometric Mg-spinel ($MgAl_2O_4$) Shocoat K-70F, −25 +5 μm (Showa-Denko, Japan). The grain sizes measured by laser diffraction were $d_{10} = 8.6$ μm, $d_{50} = 17.1$ μm, and $d_{90} = 31.7$ μm. Figure 3 shows the Mg-spinel particle morphology. The substrates were samples and interconnects made of Crofer 22 APU (ThyssenKrupp VDM, Werdohl, Germany) which is a highly corrosion resistant ferrite steel. It is frequently applied for SOFCs as it shows a thermal expansion coefficient close to that of the electrolytes. The substrates were grit blasted by corundum (size 0.06-0.1 mm) and compressed air (250 kPa). Immediately before coating, they were preheated by the plasma jet up to 500 °C.

In Table 2, the corresponding plasma spray parameters are given. In this case, the F4 gun was operated close to its power limit. In principle, the total enthalpy of the plasma gas mixture results from the enthalpies of its single components according to their molar fraction. Hydrogen shows the most considerable contribution followed by argon and helium. Furthermore, the arc is constricted by the increasing heat flow into the plasma gas when its flow is increased. As a consequence, at constant currents higher voltages are needed resulting in higher electrical input powers. This effect is increased by adding such secondary plasma gases with high thermal conductivities. Hydrogen in particular, shows a local maximum in the temperature range of its dissociation. Also helium has slightly higher thermal conductivity compared to argon. According to these characteristics, the applied plasma gas composition was chosen with regard to the basic objective of producing thin and dense coatings.

Leakage testing was done at five coated and soldered SOFC components. They were connected to a defined vacuum measuring volume and the leakage volume flow was determined based on the pressure increase. The maximum allowed leakage rate was 5 mL min^{-1} air. Furthermore the electrical resistance was measured between two bonds on both faces of the joint components. It should be higher than 1 MΩ at 5 V voltage and room temperature.

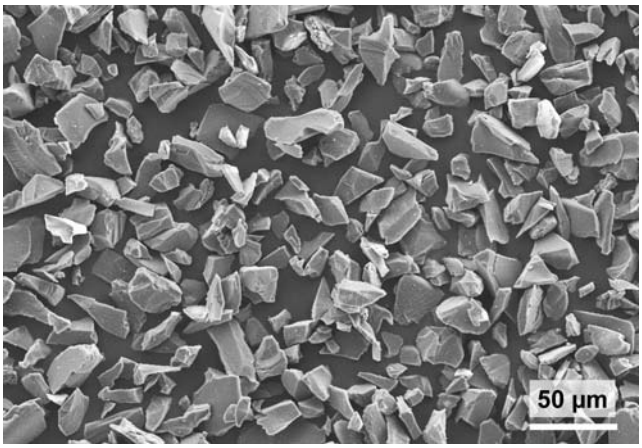

Fig. 3 Morphology of the Mg-spinel powder used for the SOFC insulating layers (SEM)

Table 2 Plasma spray parameters applied for the Mg-spinel SOFC insulating layers

Plasma gas Ar/H_2/He	30 slpm/15 slpm/5 slpm
Current, input power	730 A, 53.5 kW
Atmosphere	150 Pa Ar
Stand-off distance	800 mm

slpm, Standard liters per minute

5. Results and Discussion

5.1 Perovskites

Spraying the perovskite $Ba_{0.5}Sr_{0.5}Fe_{0.2}Co_{0.8}O_3$ material with a plasma gas composition of 80 slpm Ar and 40 slpm He yielded high particle velocities but quite low particle temperatures. Thus, the coating was not dense and some incoherent. Reducing the total plasma gas flow and increasing the helium fraction (20 slpm Ar, 40 slpm He) resulted only in a slight improvement. The use of nitrogen as secondary plasma gas (50 slpm Ar, 8 slpm N_2) showed better results regarding deposition efficiency and density of the coating. Figure 4 shows a micrograph taken by scanning electron microscope (SEM with back scattering electrons). The thickness is 75 μm.

The samples sprayed with combinations of both the secondary plasma gas species N_2 and He showed first indications of decomposition. The corresponding x-ray diffraction (XRD) patterns in Fig. 5 imply some peaks coming up in addition to the perovskite reflections. They are marked with red arrows, as they could not be

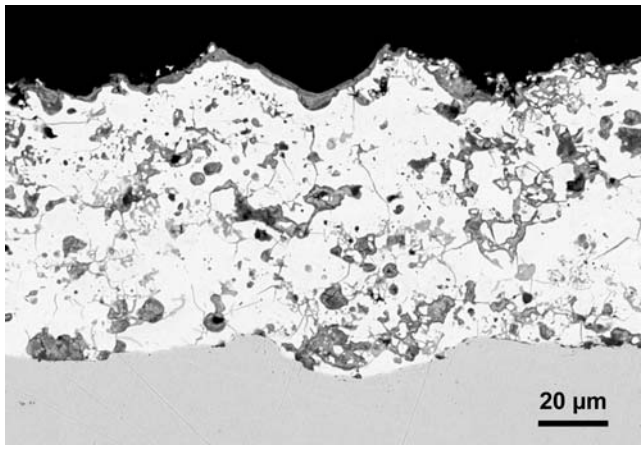

Fig. 4 Perovskite $Ba_{0.5}Sr_{0.5}Fe_{0.2}Co_{0.8}O_3$ oxygen ion conducting membrane layer as VLPPS sprayed with 50 slpm Ar and 8 slpm N_2 (SEM back scattering electron micrograph)

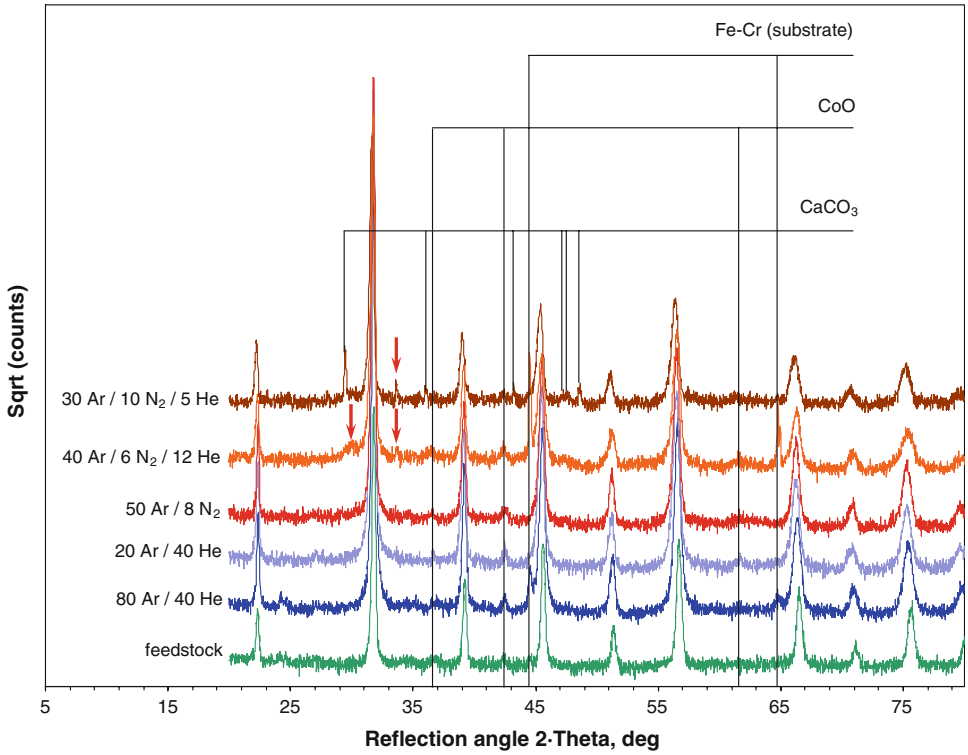

Fig. 5 XRD patterns of the perovskite $Ba_{0.5}Sr_{0.5}Fe_{0.2}Co_{0.8}O_3$ powder feedstock and of the coatings sprayed with five different plasma gas compositions. Upcoming peaks denoting decomposition products are marked with *red arrows*

clearly allocated. Probably they indicate decomposition products like BaO or $BaFe_2O_4$. Regarding the other parameters, it can be seen that a possible decomposition of the material was successfully avoided. Only some small reflections of CoO were detected which is already present in the powder feedstock. Analyzing the least dense (80 slpm Ar, 40 slpm He) and the least thick coating (40 slpm Ar, 6 slpm N_2, 12 slpm He), some Cr-Fe reflections were also found originating from the substrate. The weak $CaCO_3$ reflections are caused by a contamination at sample preparation.

These results show that for this $Ba_{0.5}Sr_{0.5}Fe_{0.2}Co_{0.8}O_3$ perovskite material there is obviously only a small gap between sufficient melting of the particles on one side and beginning decomposition of the material on the other side. With these preconditions, it seems very difficult to achieve gas-tight coatings. Since it obvious from the microstructures that the perovskite coatings sprayed within these experiments were still not gas-tight, no such measurements were performed. As a part of the ongoing work on this material a new powder batch with considerably smaller grain sizes (d_{50} approximately 10 µm) will be manufactured and tested. The process parameters will be adapted to achieve proper injection into the plasma plume and to avoid overheating of the particles.

5.2 Mg-Spinel Coatings

Figure 6 shows a micrograph taken by SEM (secondary electrons) of an as sprayed Mg-spinel SOFC insulation layer. The thickness is almost 40 µm. Some lamellae appear darker than others. This material contrast which is well known for sprayed Mg-spinel coatings was confirmed to be true and not an artifact by several images at different tilt angels. However, no differences in composition could be identified by energy dispersive-x-ray (EDX) analysis. Furthermore, the only phase which could be determined by XRD in the powder feedstock as well as in the sprayed coatings was the cubic $MgAl_2O_4$. Thus, any changes of

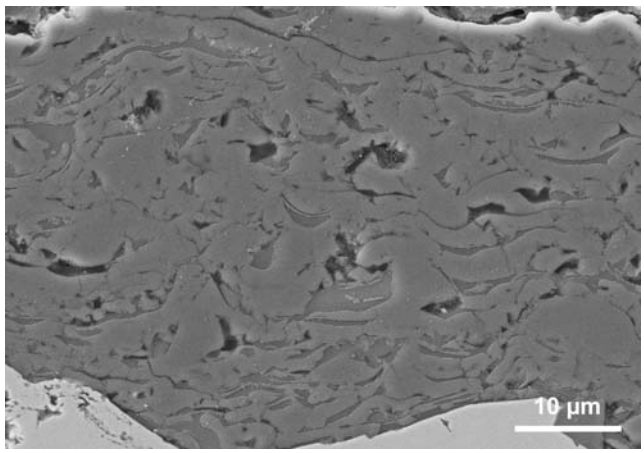

Fig. 6 Mg-spinel SOFC insulation layer as VLPPS sprayed (SEM secondary electron micrograph)

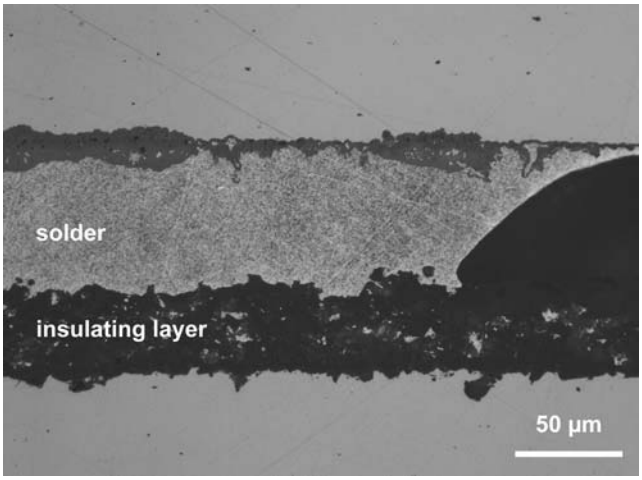

Fig. 7 Mg-spinel SOFC insulation layer as soldered (optical microscope)

composition or phases do not explain the observed color variations.

Impurities which could be found by SEM backscattering electron micrographs and EDX (not shown) were small traces of calcium silicate ($CaSiO_3$) originating from impurities of the powder. However, their locations do not correlate with the lamellae color variations. Thus, it has to be assumed that it is a preparation effect associated with hardness variations for different crystal orientations.

5.3 Solder Joints

In Fig. 7, an optical microscope micrograph of a soldered sample is given. The Ag-based solder material containing 4 mol% CuO had been applied by screen printing. The insulation layers must show an electrical resistance of at least 1 kΩ at 750 °C (~1 MΩ at testing conditions 5 V and room temperature) and gas permeability below 0.03 mL min^{-1} $part^{-1}$. Although some solder penetrated pores can be identified, the electrical resistance was determined to be 2.0 ± 0.4 MΩ. Thus, all five sprayed components met the specification. One of these five frames was also completely dense according to the requirements while the others showed too high leakage rates. The example given in Fig. 7 shows a good joint between the solder and insulation layer. However, x-ray patterns of such brazed parts which are not sufficiently dense (not shown) show that the main reasons are voids in the soldering due to locally imperfect wetting. To improve this, in the framework of the future development the composition of the solder material will be modified.

6. Summary and Conclusion

Ion conducting oxygen ion conducting membrane layers were sprayed using a spray dried $Ba_{0.5}Sr_{0.5}Fe_{0.2}Co_{0.8}O_3$ powder with the VLPPS process at 150 Pa. No hydrogen was used as secondary plasma gas to avoid decomposition due to reduction. It was found that the composition of the plasma gas considerably affects the coating properties. Obviously, for this perovskite material there is only a small gap between sufficient melting of the particles on one side and beginning decomposition of the material on the other side. Thus, further efforts have to be undertaken to achieve sufficient gas-tight coatings for gas separating membrane applications. In contrast, VLPPS-sprayed Mg-spinel SOFC insulation layers were gas-tight and showed adequate electrical resistances at a coating thickness of approximately 40 µm.

Acknowledgments

The cooperation with Dr. Uwe Maier and Dr. Thomas Kiefer, ElringKlinger AG, Dettingen/Erms, Germany in developing the SOFC insulation layers is gratefully acknowledged. This work was funded by the German Federal Ministry of Economics and Technology in the framework of the ZeuS III project. The authors also thank Andreas Hospach for his support in spraying and evaluating samples, Mark Kappertz for the metallographic preparations, Hiltrud Moitroux for taking the photo in Fig. 1, Dr. Doris Sebold for the SEM and EDX investigations (all Forschungszentrum Jülich GmbH, IEF-1), and Mierko Ziegner (ibid., IEF-2) for taking the XRD analysis.

References

1. J.-L. Dorier, M. Gindrat, C. Hollenstein, M. Loch, A. Refke, A. Salito, and G. Barbezat, Plasma Jet Properties in a New Spraying Process at Low Pressure for Large Area Thin Film Deposition, *Thermal Spray 2001: New Surfaces for a New Millennium*, C.C. Berndt, K.A. Khor, and E.F. Lugscheider, Ed., May 28-30, 2001 (Singapore), ASM International, 2001, p 759-764
2. B. Jodoin, M. Gindrat, J.-L. Dorier, C. Hollenstein, M. Loch, and G. Barbezat, Modelling and Diagnostics of a Supersonic DC Plasma Jet Expanding at Low Pressure, *International Thermal Spray Conference*, E. Lugscheider and C.C. Berndt, Ed., March 04-06, 2002 (Essen, Germany), Verlag für Schweißen und verwandte Verfahren DVS-Verlag, 2002, p 716-720
3. M. Gindrat, J.-L. Dorier, C. Hollenstein, M. Loch, A. Refke, A. Salito, and G. Barbezat, Effect of Specific Operating Conditions on the Properties of LPPS Plasma Jets Expanding at Low Pressure, *International Thermal Spray Conference*, E. Lugscheider and C.C. Berndt, Ed., March 04-06, 2002 (Essen, Germany), Verlag für Schweißen und verwandte Verfahren DVS-Verlag, 2002, p 459-464
4. C. Verdy, C. Zhang, D. Sokolov, H. Liao, D. Klein, and C. Coddet, Gas-tight Coatings Produced by Very Low Pressure Plasma Spraying, *Thermal Spray 2008: Thermal Spray Crossing Borders*, on CD-ROM, E. Lugscheider, Ed., June 02-04, 2008 (Maastricht, The Netherlands), Verlag für Schweißen und verwandte Verfahren, 2008, p 398-402
5. A. Refke, M. Gindrat, K. von Niessen, and R. Damani, LPPS Thin Film: A Hybrid Coating Technology between Thermal Spray and PVD for Functional Thin Coatings and Large Area Applications, *Thermal Spray 2007: Global Coating Solutions*, on CD-ROM, B.R. Marple, M.M. Hyland, Y.-C. Lau, C.-J. Li, R.S. Lima, and G. Montavon, Ed., May 14-16, 2007 (Beijing, China), ASM International, 2007, p 705-710
6. M. Gindrat, A. Refke, and R. Schmid, Process Characterization of LPPS Thin Film Processes with Optical Diagnostics, *Thermal*

Spray 2007: Global Coating Solutions, on CD-ROM, B.R. Marple, M.M. Hyland, Y.-C. Lau, C.-J. Li, R.S. Lima, and G. Montavon, Ed., May 14-16, 2007 (Beijing, China), ASM International, 2007, p 826-831
7. R. Vaβen and D. Stöver, Development of Thin and Gastight Ceramic Coatings by Atmospheric Plasma-spraying, *Thermal Spray 2006: Thermal Spray: Building on 100 Years of Success*, on CD-ROM, B.R. Marple, M.M. Hyland, Y.-C. Lau, C.-J. Li, R.S. Lima, and J. Voyer, Ed., May 15-18, 2006 (Seattle, USA), 2006
8. C. Zhang, H. Liao, M. Planche, C. Coddet, C.-X. Li, G.-J. Yang, and C.-J. Li, Study on Gas Permeation Behavior Through Atmospheric Plasma-sprayed Yttria Stabilized Zirconia Coating, *Thermal Spray 2008: Thermal Spray Crossing Borders*, on CD-ROM, E. Lugscheider, Ed., June 02-04, 2008 (Maastricht, The Netherlands), Verlag für Schweißen und verwandte Verfahren DVS Verlag, 2008, p 410-415
9. C. Monterrubio-Badillo, H. Ageorges, T. Chartier, J.F. Coudert, and P. Fauchais, Preparation of $LaMnO_3$ Perovskite Thin Films by Suspension Plasma Spraying for SOFC Cathodes, *Surf. Coat. Tech.*, 2006, **200**(12-13), p 3743-3756
10. A. Ansar, G. Schiller, O. Patz, J. B. Gregoire, and Z. Ilhan, Plasma Sprayed Oxygen Electrode for Solid Oxide Fuel Cells and High Temperature Electrolyzers, *8th European Solid Oxide Fuel Cell Forum*, on CD-ROM, June 30-July 04, 2008 (Luzern, Switzerland), p B1306
11. R. Henne, Solid Oxide Fuel Cells: A Challenge for Plasma Deposition Processes, *J. Therm. Spray Techn.*, 2007, **16**(3), p 381-403
12. A. Refke, G. Barbezat, D. Hawley, and R.K. Schmid, Low Pressure Plasma Spraying (LPPS) as a Tool for the Deposition of Functional SOFC Components, *Thermal Spray 2004: Advances in Technology and Application*, on CD-ROM, May 10-12, 2004 (Osaka, Japan), Verlag für Schweißen und verwandte Verfahren DVS-Verlag, 2004, Applications III, p 26-30
13. D. Stöver, D. Hathiramani, R. Vaßen, and R.J. Damani, Plasma-sprayed Components for SOFC Applications, *Surf. Coat. Tech.*, 2006, **201**(5), p 2002-2005
14. R. Vaßen, D. Hathiramani, J. Mertens, V.A.C. Haanappel, and I.C. Vinke, Manufacturing of High Performance Solid Oxide Fuel Cells (SOFCs) with Atmospheric Plasma Spraying (APS), *Surf. Coat. Tech.*, 2007, **202**(3), p 499-508
15. R. Vaßen, A. Hospach, D. Hathiramani, J. Mertens, V. Haanappel, I.C. Vinke, and D. Stöver, High Performance Solid Oxide Fuel Cells (SOFCs) Made by Atmospheric Plasma Spraying (APS), *Thermal Spray 2008: Thermal Spray Crossing Borders*, on CD-ROM, E. Lugscheider, Ed., June 02-04, 2008 (Maastricht, The Netherlands), Verlag für Schweißen und verwandte Verfahren DVS Verlag, 2008, p 110-115
16. M. Gindrat, A. Refke, and R. Damani, APS-Triplex and LPPS-Thin Film as Advanced Plasma Spraying Technologies for Industrialization of SOFC Components, *Thermal Spray 2008: Thermal Spray Crossing Borders*, on CD-ROM, E. Lugscheider, Ed., June 02-04, 2008 (Maastricht, The Netherlands), Verlag für Schweißen und verwandte Verfahren DVS Verlag, 2008, p 100-105
17. J. Arnold, S.A. Ansar, U. Maier, and R. Henne, Insulating and Sealing of SOFC Devices by Plasma Sprayed Ceramic Layers, *Thermal Spray 2008: Thermal Spray Crossing Borders*, on CD-ROM, E. Lugscheider, Ed., June 02-04, 2008 (Maastricht, The Netherlands), Verlag für Schweißen und verwandte Verfahren DVS Verlag, 2008, p 95-99
18. A. Hospach, U. Maier, and R. Vaßen, Development of a Thermally Sprayed Insulation Layer for SOFCs, *8th European Solid Oxide Fuel Cell Forum*, on CD-ROM, June 30-July 04, 2008 (Luzern, Switzerland), p A0907